Earth and Planetary Science Letters 554 (2021) 116665

Contents lists available at ScienceDirect

Earth and Planetary Science Letters

www.elsevier.com/locate/epsl

Temperature signals of ice core and speleothem isotopic records from Asian monsoon region as indicated by precipitation $\delta^{18}O$

Wusheng Yu [a,b,*], Tandong Yao [a,b], Lonnie G. Thompson [c], Jean Jouzel [d], Huabiao Zhao [a,b], Baiqing Xu [a,b], Zhaowei Jing [a], Ninglian Wang [e], Guangjian Wu [a,b], Yaoming Ma [a,b], Jing Gao [a,b], Xiaoxin Yang [a,b], Jingyi Zhang [a], Dongmei Qu [a]

[a] Key Laboratory of Tibetan Environment Changes and Land Surface Processes, Institute of Tibetan Plateau Research, Chinese Academy of Sciences, Beijing 100101, China
[b] CAS Center for Excellence in Tibetan Plateau Earth Sciences, Beijing 100101, China
[c] Byrd Polar and Climate Research Center, The Ohio State University, Columbus, OH 43210, USA
[d] Laboratoire des Sciences du Climat et de l'Environnement - IPSL, UMR 8212, CEA-CNRS-UVSQ, Gif sur Yvette, France
[e] College of Urban and Environmental Sciences, Northwest University, Xi'an 710127, China

ARTICLE INFO

Article history:
Received 21 November 2019
Received in revised form 15 October 2020
Accepted 2 November 2020
Available online 17 November 2020
Editor: Y. Asmerom

Keywords:
inverted $\delta^{18}O$ records
temperature
ice core
speleothem
Asian monsoon region

ABSTRACT

Ice cores and speleothem $\delta^{18}O$ records from Asia have been widely used as a proxy to reconstruct paleoclimate changes. However, whether those $\delta^{18}O$ records are a proxy of temperature or monsoon intensity has remained a great controversy. Generally, ice core $\delta^{18}O$ records from non-monsoon and transition regions indicate temperature, but ice core and speleothem $\delta^{18}O$ records from monsoon regions have been regarded as proxies for monsoon intensity or precipitation. Here, we address the controversy by showing three 20-yr long daily precipitation $\delta^{18}O$ ($\delta^{18}O_p$) series and 120 monthly $\delta^{18}O_p$ series based on 17461 precipitation samples throughout Asia. We find that the $\delta^{18}O_p$ signals preserved in precipitation are consistent with those in ice cores, both in the non-monsoon and monsoon regions. The results confirm previous research that ice core $\delta^{18}O$ records in the non-monsoon region provide reliable histories of surface temperature. However, ice core $\delta^{18}O$ records can still directly indicate surface temperature in the monsoon domain if winter/spring precipitation is heavy. When winter/spring precipitation is sparse, inverted ice core records show good agreement with surface temperature records. This may be due to the effect of cloud-top temperatures (which differ from surface temperatures) on summer $\delta^{18}O_p$ values. Similarly, inverted speleothem $\delta^{18}O$ records in the monsoon regions are similar to Greenland/Antarctic ice core $\delta^{18}O/\delta D$ time series and other paleotemperature records. Our findings provide a reinterpretation of Asian ice core and speleothem $\delta^{18}O$ records, and demonstrate that temperature signals have been preserved in those archives from the Asian monsoon region.

1. Introduction

The ratios of stable isotopes, ^{18}O to ^{16}O and ^{2}H to ^{1}H (expressed as $\delta^{18}O$ and δD), have been defined as "fingerprints" of water. Hence, $\delta^{18}O$ and δD are widely used to identify different moisture sources in various regions (Cobb et al., 2007), to determine various components of the hydrological cycle (Birks and Edwards, 2009), and to reconstruct paleoclimate variations, such as climatic oscillations (Dansgaard et al., 1969), general instability of past climate (Dansgaard et al., 1993), temperature (Jouzel et al., 2007), and monsoon intensity (Cheng et al., 2016) variations.

In paleoclimate studies, several long ice cores have been drilled through the Greenland and the Antarctic ice sheets from which paleotemperature records have been reconstructed (Jouzel et al., 1987; Johnsen et al., 1992; Dansgaard et al., 1993; North Greenland Ice Core Project members, 2004), with the longest continuous record covering 800 kyr (Jouzel et al., 2007). Recently, an Antarctic ice core record dating two million years has been reported, unfortunately it is only a snapshot in time and not continuous (Yan et al., 2019). Over the past 30 yrs several valuable ice core and speleothem $\delta^{18}O$ records have been recovered from throughout Asia in order to help reconstruct the regional paleoclimate (Thompson et al., 1989, 1997, 2000; Yao et al., 2007; Hou et al., 2003; Zhao et al., 2012; Wang Y. et al., 2008; Sinha et al., 2011;

* Corresponding author at: Key Laboratory of Tibetan Environment Changes and Land Surface Processes, Institute of Tibetan Plateau Research, Chinese Academy of Sciences, Beijing 100101, China.
E-mail address: yuws@itpcas.ac.cn (W. Yu).

https://doi.org/10.1016/j.epsl.2020.116665
0012-821X/

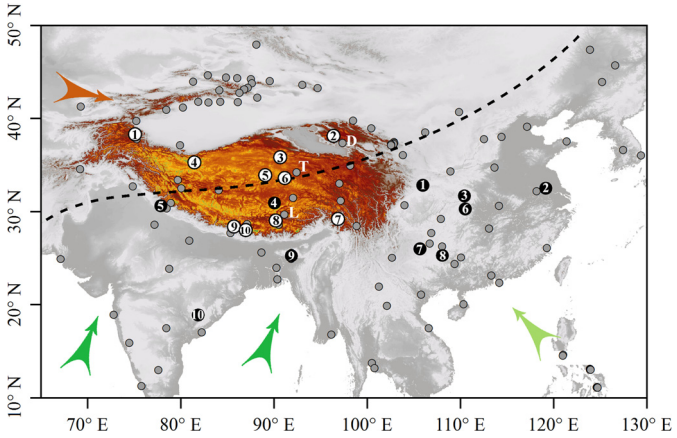

Fig. 1. Location of the ice core drilling sites (white dots), precipitation sampling stations (gray dots), and caves (black dots) in Asia. Location of the modern transition region between non-monsoon and monsoon regions is shown by a black dashed line. The numbers 1–10 in the white dots mark the locations of the ice cores listed in Supplementary Table 1. The numbers 1–10 in the black dots mark the locations of the 10 speleothems listed in Supplementary Table 2. The three gray dots marked with white letters ("D", "T", and "L") mark the locations of the stations at Delingha, Tuotuohe, and Lhasa. The other 117 precipitation sampling stations are also shown (gray dots) (see Supplementary Table 3 for details). Arrows indicate the trajectories of the westerlies (brown), the Indian monsoon (dark green, via the Arabian Sea and the Bay of Bengal) and the East Asian monsoon (light green). (For interpretation of the colors in the figure(s), the reader is referred to the web version of this article.)

Cheng et al., 2016; Kathayat et al., 2017) (Fig. 1, Supplementary Table 1, and Supplementary Table 2). Compared with the polar regions, the topographic relief and atmospheric circulation systems of Asia are more complex, and Asian ice core and speleothem $\delta^{18}O$ records reflect influences of multiple air masses and atmospheric and oceanic processes. As a consequence, the use of Asian paleoclimate $\delta^{18}O$ records as temperature proxies has long been controversial, especially in the monsoon domain. It is generally believed that ice core $\delta^{18}O$ time series from the non-monsoon region and the transitional region between the monsoon and non-monsoon regions record temperature change (Thompson et al., 1989, 1997, 2018; Yao et al., 2007; Wang et al., 2003; Tian et al., 2006; Kang et al., 2010), but within the monsoon domain $\delta^{18}O$ records are often considered to be a monsoon intensity (precipitation amount) signal (Hou et al., 2003; Zhao et al., 2012; Yuan et al., 2004; Wang Y. et al., 2008; Cai et al., 2010; Sinha et al., 2011; Cheng et al., 2016; Kathayat et al., 2017) or a temperature signal (Zhao et al., 2017) (Supplementary Fig. 1). It is evident that the signals preserved in ice cores from the monsoon region are more difficult to interpret. For example the Noijin Kangsang ice core $\delta^{18}O$ records from the Lhagoi Kangri mountains (Zhao et al., 2012) (Fig. 1) are inversely correlated with the Northern Hemisphere temperature (NHT) anomalies (Supplementary Figs. 1, 2), and the East Rongbuk ice core $\delta^{18}O$ records from Mt. Everest appear to record Indian monsoon precipitation (Hou et al., 2003). However, the Dasuopu ice cores from Mt. Xixiabangma (located near Mt. Everest) (Thompson et al., 2000) and the Zuoqiupu ice core from the southeastern margin of the Himalayas (Zhao et al., 2017) are considered to be indicators of temperature on interannual time scales (Supplementary Fig. 2). This controversy is because the factors affecting variations in stable isotopes in ice cores and speleothems are unclear.

Previous studies have emphasized that systematic variabilities, such as in temperature, humidity, and pressure, strongly affect $\delta^{18}O$ values in precipitation (Dansgaard, 1964). Moreover, the seasonal shifts of moisture sources can play a key role in the seasonal cycle of precipitation $\delta^{18}O$ (Cobb et al., 2007). In addition, intensified meridional and zonal circulation can modify $\delta^{18}O$ values in precipitation (Birks and Edwards, 2009). Recent studies have demonstrated that precipitation $\delta^{18}O$ can reflect proportions of convective and stratiform precipitation and is negatively correlated with stratiform fractions, especially in the tropical regions (Aggarwal et al., 2016). Because the signals of ice cores and speleothems are related to those of ancient precipitation, understanding the key influences that dominate precipitation $\delta^{18}O$ variations is very important for the interpretation of these paleoclimatic records.

Here, we attempt to address the controversy mentioned above from the perspective of $\delta^{18}O$ records from daily precipitation samples collected over 20 yrs at three meteorological stations located at Delingha, Tuotuohe, and Lhasa of the Tibetan Plateau Network for Isotopes in Precipitation (TNIP) (Fig. 1). To achieve this goal, we first prove that low-altitude $\delta^{18}O$ values from precipitation are consistent with those from high-altitude ice cores, then identify the consistent relationship between $\delta^{18}O$ and different meteorological parameters such as temperature, precipitation amount, and relatively humidity in the different regions (monsoon, transition, and non-monsoon regions), and finally, demonstrate that the temperature signals were preserved in the $\delta^{18}O$ records (especially inverted $\delta^{18}O$ records) from Asian ice cores and speleothems.

2. Materials and methods

2.1. Observed $\delta^{18}O$ database

In the TNIP project, samples from each precipitation event were collected immediately after the event from a rain gauge. Rainfall samples were collected immediately after each event from a rain gauge with a collection funnel. Note a plastic table tennis ball was placed in the collection funnel to seal the collector bottle against evaporation and debris. The samples were transferred into 15 mL plastic bottles, sealed with screw caps, and wrapped with parafilm to prevent sample loss and evaporation prior to analysis. Solid precipitation samples were collected on clean porcelain plates, put into clean plastic bags, and sealed. The solid samples were processed using the same methodology as rainfall samples after they melted at room temperature. All samples were stored below freezing until being analyzed. Additionally, the duration of each precipitation event, surface temperature (T), relative humidity (RH), and precipitation amount (P) were recorded as samples were collected (Yu et al., 2017). In this study, we collected and measured 11095 precipitation event samples from 21 stations, including the three 20-yr long observation stations of Lhasa, Tuotuohe, and Delingha (1540, 1869, and 2040 samples, respectively) (Supplementary Table 3).

Precipitation samples collected prior to 2004 were analyzed at the State Key Laboratory of Cryosphere (Lanzhou), Chinese Academy of Sciences, using a MAT-252 mass spectrometer with a precision of ±0.2‰ for $\delta^{18}O$ values. Precipitation samples collected in 2005–2008 and in 2009–2014 were measured at the Key Laboratory of Tibetan Environmental Changes and Land Surface Processes (Beijing), Chinese Academy of Sciences, using a MAT-253 mass spectrometer and a Picarro-L2130i Cavity Ring-down Spectroscopy with precisions of ±0.1‰ and ±0.1‰ for $\delta^{18}O$ values, respectively (Yao et al., 2013). All the data of the measured precipitation are expressed as parts per thousand of their deviation relative to the Vienna Standard Mean Ocean Water (VSMOW or VSMOW2). The detailed sampling and measurement procedures were published by Yao et al. (2013).

We also selected some monthly precipitation $\delta^{18}O$ data from 69 observation stations of the International Atomic Energy Agency/World Meteorological Organization (IAEA/WMO) Global Network of Isotopes in Precipitation (GNIP) (available at https://www.iaea.org/services/networks/gnip). Similar to the TNIP, rainfall samples were collected from a rain gauge. Large collection bottles were needed to collect monthly samples. The rain gauge was read and emptied

as soon as possible in the morning following each precipitation event. After reading and recording the volume, the collected water was poured into the accumulation bottle, which was tightly sealed and stored in a refrigerator. The samples were analyzed mainly in the IAEA's Isotope Hydrology Laboratory in Vienna, but were also measured in cooperating laboratories. The measurements reported in GNIP have a long term precision of about ±0.1‰ for $\delta^{18}O$ values at one standard deviation (IAEA/WMO, 2018). In addition, some precipitation $\delta^{18}O$ data at 30 observation stations collected by previous studies (Liu et al., 2007; Pang et al., 2011; Duan et al., 2016; Li Z. et al., 2016; Guo et al., 2017; Wang et al., 2016) were used. The data from the 120 stations present a good representation of precipitation $\delta^{18}O$ ($\delta^{18}O_p$) changes in the non-monsoon, transition, and monsoon regions (Yao et al., 2013) (Fig. 1, Supplementary Fig. 3, Supplementary Table 3).

2.2. Retrieved $\delta^{18}O$ database

In addition to the observed precipitation $\delta^{18}O$ dataset, we also used water vapor isotopic data (δD) derived from Tropospheric Emission Spectrometer (TES). The TES instrument is a Fourier transform spectrometer onboard the National Aeronautics and Space Administration (NASA) Aura satellite, which was launched in 2004 and ended surveillance in 2018. It captured the global vertical profiles of water vapor and its isotopes by measuring radiances in the range of 1200–1350 cm^{-1} at a spectral resolution of 0.1 cm^{-1} (Worden et al., 2011). The detailed retrieval procedures have been described elsewhere (Worden et al., 2011). The water vapor δD data were provided by NASA Langley Research Center Atmospheric Science Data Center (available at https://tes.jpl.nasa.gov/data). We used the retrieved H_2O and HDO of version 6 Lite level 2 H_2O and HDO nadir retrievals from three stations (Lhasa, Tuotuohe and Delingha) and a region covering 10°N to 25°N and 65°E to 130°E during 2006–2009 because of good measuring continuities. To ensure data quality, we omitted data whose species retrieval quality was 0 and the degrees of freedom for signals were less than 0.5. To better compare with the observed precipitation $\delta^{18}O$ data, the δD data were used to calculate $\delta^{18}O$ using the equation $\delta D = 8.0\delta^{18}O + 10$ (Craig, 1961).

2.3. Simulated $\delta^{18}O$ database

In this study, the simulations of the $\delta^{18}O$ database including the stable oxygen isotopic ratios in water vapor ($\delta^{18}O_v$) at 500 hPa and the $\delta^{18}O_p$ were performed by the ECHAM5-wiso model (Mutz et al., 2016). The ECHAM5-wiso is an atmospheric general circulation model enhanced by stable water isotope diagnostics (Werner et al., 2011). The model is run for modern conditions with a horizontal spatial resolution of 1.8° × 1.8° and 19 vertical levels (up to 10 hPa). Subgrid scale orography parameterization has been implemented in ECHAM5-wiso to better quantitatively understand the local climatic and topographic controls on precipitation $\delta^{18}O$ (Mutz et al., 2016). Recent studies have demonstrated that the simulation with ECHAM5-wiso on the Tibetan Plateau captures the corresponding observations very well (Li J. et al., 2016). The detailed ECHAM5-wiso simulation procedures have been described elsewhere (Werner et al., 2011; Mutz et al., 2016). The standard climatological reference period (1979–1999) modeling outputs are used in this study.

2.4. Meteorological and other related data

During the precipitation sampling, we recorded the duration of each precipitation event, surface temperature, relative humidity, and precipitation amount. To compare the seasonal variations and annual trends of precipitation amounts at the three sampling stations with those at the ice core drilling sites, we used the precipitation data observed by the Tropical Rainfall Measuring Mission (TRMM) (available at: https://pmm.nasa.gov/data-access/downloads/trmm). In addition, in order to discuss the relationships between cloud-top temperature (CTT) and the precipitation $\delta^{18}O$, we used the International Satellite Cloud Climatology Project (ISCCP) D1 and D2 products (cloud-top temperature), which were obtained from NASA Goddard Institute for Space Studies (available at: https://eosweb.larc.nasa.gov/project/isccp/isccp_table).

2.5. The iLOVECLIM Earth system model

As a three-dimensional Earth system model, the LOch-Vecode-Ecbilt-CLio-agIsM (LOVECLIM) model has a simpler representation of physical processes, although its resolution is coarser than state-of-the-art climate General Circulation Models (GCMs). Hence, LOVECLIM is much faster than GCMs (Goosse et al., 2010). The iLOVECLIM model is a code fork of the LOVECLIM-1.2 climate model, with the atmosphere, ocean, sea ice and vegetation components interactively coupled (Roche, 2013).

In our study, the annual mean atmospheric temperature and annual mean precipitation $\delta^{18}O$ data over the regions (~17°–33°N and 87°–116°E) during the past 150,000 yrs, simulated by the iLOVECLIM1.2 model, were obtained from Caley et al. (2014). The orbital configuration is calculated from Berger (1978) with constant year 1950. The run is performed using present day land-sea mask, freshwater routing and interactive vegetation (Roche, 2013). The temperature is driven by both natural (insolation) and anthropogenic (greenhouse gas) forcings (Yin and Berger, 2010). With regards to the precipitation $\delta^{18}O$ data, the main development lies in the atmospheric component in which evaporation, condensation and existence of different phases (liquid and solid) all affect the isotopic conditions of the precipitation $\delta^{18}O$ data (Roche, 2013). The precipitation $\delta^{18}O$ data were corrected from the ice-sheet contribution to the global seawater $\delta^{18}O$ data over the last 150,000 yrs (Caley et al., 2014).

2.6. Statistical analysis

All statistical analyses were performed on IBM SPSS Statistics version 19.0 (IBM Corp. Armonk, NY, USA). Least squares linear regression was used to determine if there was a linear correlation between independent variables and dependent variables. Relationships between variables were assessed using standard bivariate procedures. A value of $p < 0.05$ is considered significant.

3. Results

3.1. Two hypotheses were tested

Before the controversy can be resolved, it is first necessary to prove that low-altitude $\delta^{18}O_p$ values are consistent with those from high-altitude ice cores. Here we proposed two hypotheses: i) the signal consistency (i.e., the temporal trends in ice core $\delta^{18}O$ records at high altitude should be similar to those in $\delta^{18}O_p$ records at low altitude); and ii) the consistency of precipitation amount patterns (i.e., the seasonal variations and annual trends of precipitation amounts at the three sampling stations should be similar to those at the ice core drilling sites). To test the first hypothesis, we compared the $\delta^{18}O$ records from the three precipitation sampling stations of Delingha, Tuotuohe, and Lhasa with those from the adjacent three ice cores (from north to south, they were Dunde, Puruogangri, and Noijin Kangsang ice cores, the distances between the ice core drilling sites and adjacent sampling stations

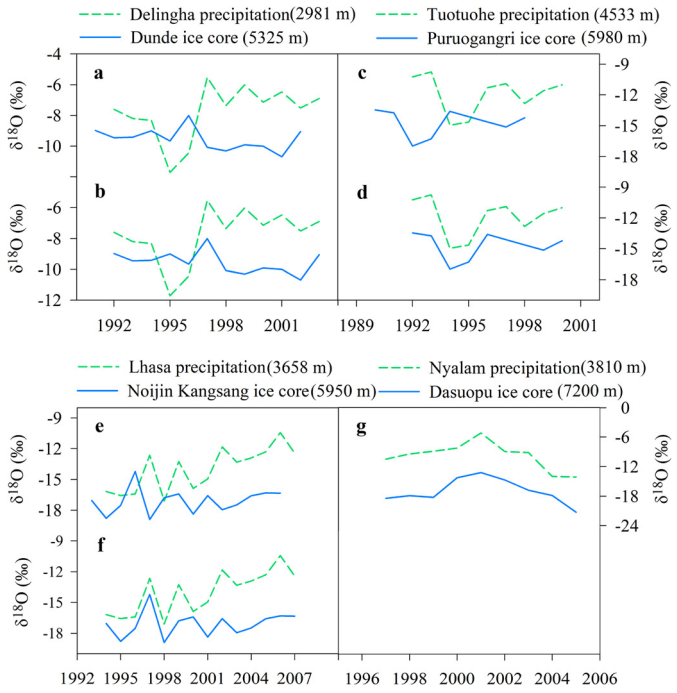

Fig. 2. Comparisons of $\delta^{18}O$ records from four ice cores (solid blue lines) and nearby precipitation sampling stations (dashed green lines). The blue and green lines indicate $\delta^{18}O$ records in ice cores of Dunde (Takeuchi et al., 2009), Puruogangri (Yao et al., 2007), and Noijin Kangsang (Zhao et al., 2012) and precipitation of Delingha, Tuotuohe, and Lhasa, which represent, in order, the non-monsoon, transition and monsoon regions, respectively. Note that (a), (c), and (e) show the raw data, and ice core $\delta^{18}O$ records were moved one year backward in (b), (d), and (f). In addition, in the monsoon region, the $\delta^{18}O$ changes in Dasuopu ice core (Thompson et al., 2000; Wang P. et al., 2008) and Nyalam precipitation are also shown (g). Their similar changes indicate no dating error for the Dasuopu ice core records. The station/ice core elevations are also shown in brackets. $\delta^{18}O$ is reported as per mil deviations from VSMOW or VSMOW2.

are 116.3 km, 311.5 km, 111.7 km in order). In addition, it is important to note that the absolute values of the $\delta^{18}O_p$ records and ice core $\delta^{18}O$ records are different due to the elevation and precipitation phase differences. If we exclude the influence of the ice core dating error by moving one year backward for the ice core $\delta^{18}O$ record, the trends of the three-site $\delta^{18}O_p$ records will be similar as those of the adjacent ice core $\delta^{18}O$ records (Fig. 2a-2f). The adjusted $\delta^{18}O$ records in the Puruogangri (Yao et al., 2007) (Fig. 2d) and Noijin Kangsang (Zhao et al., 2012) (Fig. 2f) ice cores, and the raw $\delta^{18}O$ data in the Dasuopu ice core (Fig. 2g) are positively correlated with those in precipitation, with a sample size (n) of 9, 14, and 9, a correlation coefficient (r) of 0.93, 0.60, and 0.76, within a 0.01, 0.05, and 0.05 confidence level (p), respectively. Note the positive relationship between the adjusted $\delta^{18}O$ record in the Dunde ice core (Takeuchi et al., 2009) and $\delta^{18}O$ in the Delingha precipitation (Fig. 2b) is weak ($r = 0.2$) due to the uncompleted precipitation sampling in 1995. This indicates that the signals of the low-altitude $\delta^{18}O_p$ records are consistent with those captured by the high-altitude ice core $\delta^{18}O$ records, and the low-altitude $\delta^{18}O_p$ records can represent the adjacent high-altitude ice core $\delta^{18}O$ records. The same is true for the low-altitude $\delta^{18}O_p$ records at Nyalam, located on the south slope of the Himalayas and the nearby Dasuopu ice core $\delta^{18}O$ record (Thompson et al., 2000; Wang P. et al., 2008) (the distance between the ice core-station is 35.6 km) (Fig. 2g). Note that the result of $\delta^{18}O_p$ at Delingha in 1995 was not consistent with the corresponding Dunde ice core records, possibly because some of the precipitation samples at Delingha in that year were not obtained.

To verify the consistency of mass changes, we compared the precipitation amounts from the three sampling stations (Delingha, Tuotuohe, and Lhasa) to those from the corresponding adjacent ice core drilling sites (Dunde, Puruogangri, and Noijin Kangsang ice cores). It was expected that the overall trend of precipitation amount between the low-altitude stations and the high-altitude drilling sites would be similar, whether on monthly or annual time scales. First, we compared the precipitation amounts observed at the sampling stations ($P_{station}$) with those observed by Tropical Rainfall Measuring Mission (TRMM) at the sampling stations (P_{TRMM}). The results showed that at the low-altitude sampling stations, the trends of the TRMM and surface observations were highly similar, whether for the monthly changes (with a correlation coefficient of 0.51–0.89, within a 0.05 and 0.01 confidence level) (Supplementary Fig. 4, Supplementary Table 5) or for the annual changes (with a correlation coefficient of 0.80–0.97, within a 0.01 confidence level) (Supplementary Fig. 5, Supplementary Table 6). Thus, we believe that the TRMM results can capture the monthly and annual patterns of precipitation in Asia. Second, we compared the TRMM precipitation records at the sampling stations with those at the corresponding adjacent ice core drilling sites. On the whole, whether considering the monthly patterns (Supplementary Fig. 4) or the annual changes (Supplementary Fig. 5), the fluctuations of precipitation amounts at low-altitude TRMM were similar to those at the corresponding adjacent ice core drilling sites. Therefore, we believe that the change in trends of precipitation amount at low altitude can indicate those at the adjacent high altitude.

The consistencies between the temporal variations of the $\delta^{18}O$ records and precipitation amounts at low and high altitudes demonstrate that the low-altitude $\delta^{18}O_p$ time series can record the corresponding adjacent ice core $\delta^{18}O$ signals at high altitude. This results from the fact that water isotope fractionation at different altitudes is subject to the same isotope fractionation mechanism. As an air mass follows a trajectory from its vapor source region to higher latitudes, it cools and loses its water vapor along the way as precipitation, a process called 'rainout' (Dansgaard, 1964; Clark and Fritz, 1997), which can be expressed by the Rayleigh distillation:

$$R = R_0 f^{(\alpha-1)}$$

where R_0 and R are the initial isotope ratio of the vapor and the isotope ratio after rainout, respectively. The quantity f is the residual fraction of vapor in the air mass, and α is the equilibrium isotopic fractionation factor between vapor and liquid water at the in-cloud temperature. For $\delta^{18}O$, $\ln\alpha = 1.137/(T+273.16)^2 \times 10^3 - 0.4156/(T+273.16) - 2.0667 \times 10^{-3}$) (Majoube, 1971). It is apparent that temperature is the primary driver of rainout. Hence, the $\delta^{18}O$ values of rain or snow are mainly related to the condensation temperature (Dansgaard, 1964). Both rain and snow is subject to Rayleigh distillation with slightly different isotopic fractionation factors.

3.2. Consistent relationships between $\delta^{18}O_p$ and temperature

If $\delta^{18}O_p$ can be considered as a good indicator of temperature, humidity, or precipitation amount within each region, it should meet the criterion of a significant relationship between the isotopic values and these parameters across different time scales (daily, monthly, annual). If the relationships between the isotopic values and any parameter across different time scales in any region can not maintain consistent positive or inverse correlations, they do not meet this criterion. Our findings show that the $\delta^{18}O_p$ values are positively correlated with surface temperature (i.e., temperature effect) in the non-monsoon and transition regions on different

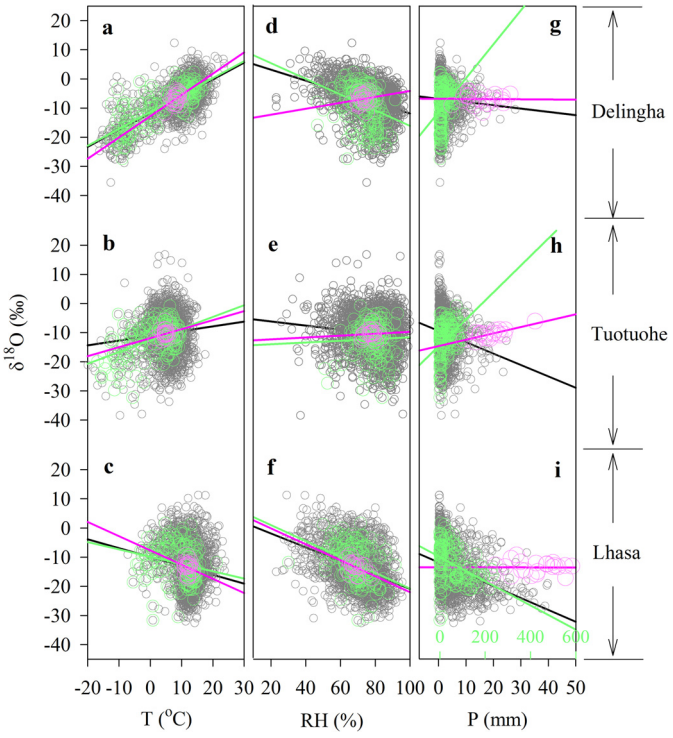

Fig. 3. The relationships $\delta^{18}O_p$–T, $\delta^{18}O_p$–RH, and $\delta^{18}O_p$–P at Delingha (a, d, and g), Tuotuohe (b, e, and h) and Lhasa (c, f, and i) on the different time scales in 1991–2014. The gray, green, and pink legends indicate the relationships on the daily, monthly and annual time scales, respectively. On the different time scales, the correlation $\delta^{18}O_p$–T is consistent in each region (the positive correlation is consistent in the non-monsoon and transition regions, and the inverse correlation is consistent in the monsoon region), but the relationships $\delta^{18}O_p$–RH and $\delta^{18}O_p$–P are not consistent in either the non-monsoon or transition region (see Supplementary Table 4 for details). $\delta^{18}O$ is reported as per mil deviations from VSMOW or VSMOW2.

time scales, with a correlation coefficient of 0.11–0.80, within a 0.05 or 0.01 confidence level (Note the positive correlation for the Tuotuohe station on annual time scale is weak, it may be because the sample number is very small). In the monsoon region a consistent but inverse correlation between $\delta^{18}O_p$ values and surface temperature exists on different time scales (defined as "inverse temperature effect" in this text), with a correlation coefficient of −0.16–−0.22, within a 0.01 confidence level (Note the inverse correlation for the Lhasa station on annual time scale is also weak, it may be because the sample number is as small as 22) (Fig. 3, Supplementary Table 4). Thus, we argue that although $\delta^{18}O_p$ measurements and ice core $\delta^{18}O$ records from the non-monsoon and transition regions can directly reflect temperature, they can "inversely" reflect the temperature in the monsoon region. However, there is not a consistent relationship between $\delta^{18}O_p$ and precipitation amount (or humidity) within or between the regions (Fig. 3, Supplementary Table 4). Note that although the $\delta^{18}O$ in the monsoon region is significantly and positively correlated with precipitation amount on daily and monthly time scales, the $\delta^{18}O$ – P annual time scale correlation in the monsoon region is not significant (Fig. 3, Supplementary Table 4). Similarly, although there is a consistent relationship between $\delta^{18}O$ and RH in the monsoon region, the $\delta^{18}O$ – RH correlations in the transition and non-monsoon regions on different time scales are not consistent. Hence, there is a degree of uncertainty over whether $\delta^{18}O$ in either precipitation or ice cores or other sediment archives (such as speleothems) can be used as a proxy for precipitation amounts or relative humidity.

4. Discussion

4.1. Temperature signals preserved in Asian ice cores

The positive correlations are significant between surface temperature and 10 representative ice core $\delta^{18}O$ records (Supplementary Fig. 1) in the non-monsoon and transition regions (with a correlation coefficient of 0.16–0.78, within a 0.05 or 0.01 confidence level); however, correlations in the monsoon region are not consistent. Significant positive correlations occur for Dasuopu (Thompson et al., 2000) and Zuoqiupu (Zhao et al., 2017) ice cores, while there is a significant negative correlation between temperature and the Noijin Kangsang ice core (with a correlation coefficient of −0.24, within a 0.01 confidence level) (Zhao et al., 2012). The correlation with the East Rongbuk ice core is not significant; however, the negative correlations between the 5-yr running means of $\delta^{18}O$ values from the East Rongbuk ice core and the NHT during 1850-1898 and 1899-1997 are significant, with a correlation coefficient of −0.51 and −0.23, within a 0.05 and 0.01 confidence level, respectively (Hou et al., 2003) (Supplementary Fig. 2, Supplementary Table 1). Because the strong Asian summer monsoon and convection results in relatively low $\delta^{18}O_p$ values in summer (Yu et al., 2017), the trends of low summer $\delta^{18}O_p$ values (Fig. 4g) are opposite to those of surface temperatures (Fig. 4c), although the pre-monsoon $\delta^{18}O_p$ values and surface temperatures gradually increase synchronously (Fig. 4g, 4c). Therefore, in the monsoon region it is necessary to consider two cases involving either heavy or sparse precipitation in winter/spring (Supplementary Fig. 6). When the precipitation in winter/spring is heavy, temperature and $\delta^{18}O$ are more closely linked both in precipitation and in the ice core records. For example, the meteorological stations at Purang and Nyalam record heavy winter/spring precipitation (Supplementary Fig. 6A) due to the favorable local topographic conditions that interact with the western disturbances (Pang et al., 2014). Hence, the nearby Dasuopu ice core $\delta^{18}O$ record may be used as a proxy for temperature (Thompson et al., 1997). Another good example is the Zuoqiupu ice core (Zhao et al., 2017), which is located in the monsoon region and is also characterized by heavy winter/spring precipitation as shown by the precipitation records from Bomi and Zayu (Supplementary Fig. 6D). Moreover, the positive correlation between $\delta^{18}O_p$ values and surface temperature before the onset of the monsoon in this region (Yu et al., 2016) supports the conclusion that the temperature signal is preserved in the nearby Zuoqiupu ice core (Zhao et al., 2017).

In regions where the winter/spring precipitation is sparse, glaciers receive proportionately more snow in the summer and thus show more of an "inverse" temperature signal that results from the negative correlation between summer $\delta^{18}O_p$ values and surface temperature (Fig. 4c, 4g). The precipitation at the meteorological stations at Lhasa and Nagarze, near the Noijin Kangsang ice core site, falls mainly in summer (Supplementary Fig. 6C), which results in a negative correlation between the Noijin Kangsang ice core $\delta^{18}O$ record (Zhao et al., 2012) and the NHT anomalies back to 1850 (Supplementary Fig. 2). This is also observed for the correlation between the East Rongbuk $\delta^{18}O$ record (Hou et al., 2003) from a glacier that also receives less winter/spring than summer precipitation as indicated by the Tingri and Pagri meteorological stations (Supplementary Fig. 6B).

Since these ice core $\delta^{18}O$ records in the monsoon region with sparse winter/spring precipitation are inversely correlated with the NHT anomalies (Supplementary Fig. 2), we inverted their time series and compared them with the relevant instrumental records (Supplementary Fig. 7). The results are mixed. On the one hand, the inverted whole East Rongbuk record (Hou et al., 2003) and the new Noijin Kangsang record (Zhao et al., 2012) (moved one year backward and then inverted) before 1989 are similar to the NHT

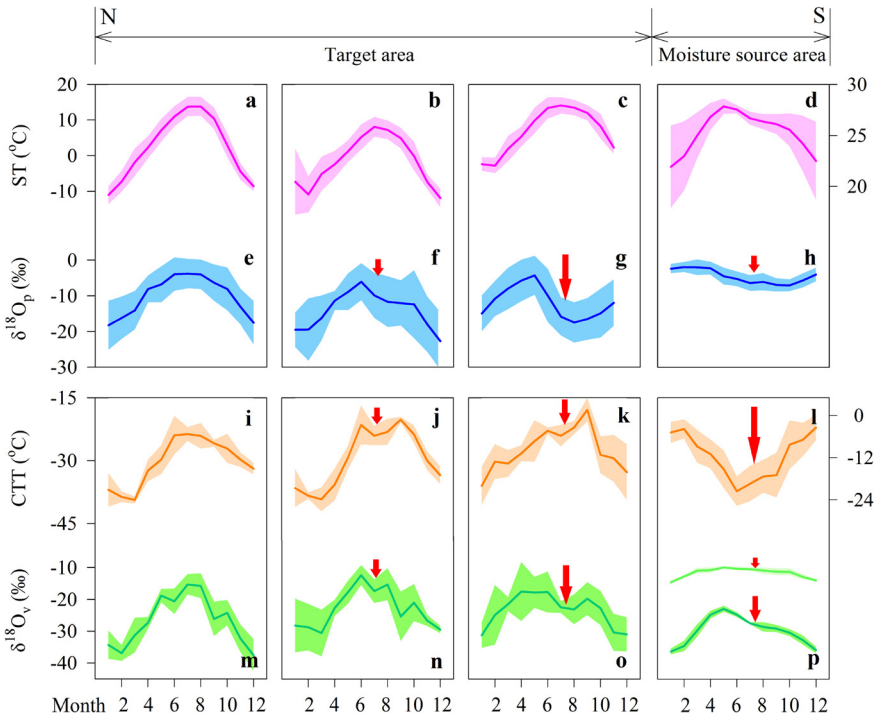

Fig. 4. Seasonal changes in surface temperature (ST, pink) and $\delta^{18}O_p$ (blue) at Delingha (a, e), Tuotuohe (b, f), and Lhasa (c, g), from 1991–2014, and the moisture source area (10°–25°N and 65°–130°E) (d, h) from 1961-2016. Seasonal changes in the cloud-top temperature (CTT, yellow) and $\delta^{18}O_v$ (green) over Delingha (i, m), Tuotuohe (j, n), and Lhasa (k, o) in the target area and the moisture source area (l, p) from 2006–2009. The shading in each panel indicates standard deviation. The red arrows mark the relatively low values in the summer. STs at the three stations were derived from instrumental data, but surface temperatures (including sea surface temperatures) over the moisture source area are from NCEP reanalysis-derived data. Note that the $\delta^{18}O_v$ variations of near surface water vapor over the moisture source area (p, light green line) are very slight. $\delta^{18}O$ is reported as per mil deviations from VSMOW or VSMOW2.

since 1850. The 5-yr running $\delta^{18}O$ record of East Rongbuk ice core is negatively correlated with the NHT over the periods of 1850-1898 and 1899-1997, with a correlation coefficient of −0.51 and −0.23, with a confidence level of 0.01 and 0.05, respectively. The new Noijin Kangsang record before 1989 is significantly correlated with the NHT, with a correlation coefficient of −0.27 and a 0.01 confidence level. However, part of the new the Noijin Kangsang ice core $\delta^{18}O$ record after 1989 was still abnormal (marked by a green box). The reason for the discrepancy remains unclear. It may be related to the abnormal local circulation (Gao et al., 2016), but further study is required to determine why the trend seems to reverse in the most recent part of the record. Interestingly, the higher frequency fluctuations of the inverted $\delta^{18}O$ record from the Noijin Kangsang ice core over the period 1993-2004 are still similar to those of the NHT, with a correlation coefficient of −0.80, within a 0.05 confidence level (Supplementary Fig. 8). Hence, we argue that the ice core $\delta^{18}O$ records in the monsoon region with sparse winter/spring precipitation can "inversely" indicate the surface temperature changes.

4.2. Temperature signals preserved in Asian speleothems

The assumption that the speleothem $\delta^{18}O$ records ($\delta^{18}O_s$) can be used as a paleoclimate proxy requires that the speleothem $\delta^{18}O$ records inherit the signals of $\delta^{18}O$ in precipitation ($\delta^{18}O_p$) outside the caves. Therefore, we can determine that the speleothem $\delta^{18}O$ records indicate temperature (or precipitation), if the precipitation $\delta^{18}O$ records outside the caves capture the temperature (or precipitation) signal. In Section 3.2, we have already demonstrated that there is not a consistent relationship between $\delta^{18}O_p$ and precipitation amount within or between the regions of the monsoon, transitional, and non-monsoon regions. The result suggests speleothem $\delta^{18}O$ records do not consistently reflect changes in precipitation amount. Previous studies also argued that speleothem $\delta^{18}O$ records in East Asia can not indicate the changes in annual precipitation (or summer precipitation) based on the relationship between precipitation amount and speleothem $\delta^{18}O$ records on annual, decadal and orbital time scales (Chen et al., 2016; Rao et al., 2016; Liu et al., 2020). In this study, we found precipitation $\delta^{18}O$ records outside the caves in the Asian monsoon region are negatively correlated with surface temperature. Hence, the inverted speleothem $\delta^{18}O$ records from the Asian monsoon region may also indicate temperature.

To demonstrate this conclusion, we firstly compared the inverted speleothem $\delta^{18}O$ curves of Jhumar-Wah caves in the South Asian monsoon region (Sinha et al., 2011), and of Zhijin (Kuo et al., 2011), Dongge (Cheng et al., 2016), and Dayu (Tan et al., 2009) caves in the East Asian monsoon region with sparse winter/spring precipitation with the NHT curve during 1850–2010 (Supplementary Fig. 9). The results show that the composite $\delta^{18}O_s$ record from Jhumar and Wah Shikar caves is significantly correlated with the NHT over the periods of 1850–2007, with a correlation coefficient of −0.40, within a 0.01 confidence level. The speleothem $\delta^{18}O$ record from Zhijin cave is negatively correlated with the NHT over the periods of 1850–1942 and 1943–1997, with a correlation coefficient of −0.43 and −0.3, within a 0.01 and 0.05 confidence level, respectively. For Dongge and Dayu caves, the trends of the inverted speleothem $\delta^{18}O$ curves are very similar to those of the NHT curve, with a correlation coefficient of −0.48 and −0.24, within a 0.05 and 0.05 confidence level, respectively, except part of the speleothem $\delta^{18}O$ records from Dongge cave after 1954 and from Dayu cave after 1976 are still abnormal (marked by a green box). The results indicate that the inverted speleothem $\delta^{18}O$ records from the Asian monsoon region may reflect changes in surface temperature.

During the last 2000 yrs, we also found that the inverted speleothem $\delta^{18}O$ record from Sahiya cave (Kathayat et al., 2017) and the composite $\delta^{18}O$ record from Jhumar and Wah Shikar caves

(Sinha et al., 2011) from the South Asian monsoon region, agree with the Northern Hemisphere and Northern Hemisphere extratropical temperature anomalies (Moberg et al., 2005; Christiansen and Ljungqvist, 2012), with a correlation coefficient of −0.22 and −0.15, within a 0.01 and 0.01 confidence level, respectively (Supplementary Fig. 10) (Note these r values are lower than the correlation observed from Jhumar-Wah, Zhijin, and Dongge Caves). In the East Asian monsoon region, during the last 2000 yrs, the trends of the inverted speleothem $\delta^{18}O$ record from Lianhua (Cosford et al., 2009) and Heshang (Hu et al., 2008) caves are also similar to those of the NHT (Supplementary Fig. 11). The Heshang speleothem $\delta^{18}O$ record is negatively correlated with the NHT during 0-1980, with a correlation coefficient of −0.10, and a confidence level of 0.01. The negative relationship between the Lianhua speleothem $\delta^{18}O$ record and the NHT during 0-1997 is also significant, with a correlation coefficient of −0.14, within a 0.05 confidence level. Clearly, those r values are close to zero indicating that the relationships only account for a small amount of the variance. We do not rule out that the Asian summer monsoon (ASM) intensity can be contributing to the variance. It is necessary to discuss the relationships between the ASM intensity and speleothem $\delta^{18}O$ records in our future studies.

In addition, we extrapolated further our findings over the longer timescales. One example is in the East Asian monsoon region, we found that an inverted speleothem $\delta^{18}O$ record (Hulu, Dongge and Sanbao caves) (Cheng et al., 2016) is similar to surface temperature over the region in which the caves are located (∼17°–33°N and 87°–116°E) as simulated by the iLOVECLIM model during periods of 8-73 and 124-150 kyr BP, with a correlation coefficient of −0.69 and −0.70, within a 0.01 and 0.01 confidence level (Caley et al., 2014) (Supplementary Fig. 12). Those results indicate that the inverted speleothem $\delta^{18}O$ records from the Asian monsoon region can capture temperature signal. Note there are still some periods where the temperature to $\delta^{18}O$ records do not agree (Supplementary Figs. 10 and 12). It may be because the precipitation patterns during those periods do not conform with the above assumption that the speleothems receive heavy summer precipitation and sparse winter/spring precipitation.

As mentioned in Cheng et al. (2019), before the data processing and comparison of the Asian monsoon (Chinese speleothem $\delta^{18}O$) and Antarctic temperature (ice core δD) records, it was difficult to imagine that there exists a close internal relationship between the Antarctic temperature and Chinese speleothem $\delta^{18}O$ records, because the two records are so distant. The relationship can be described as: $\delta^{18}O_{\text{Chinese speleothem}} - \text{Insolation}_{\text{July 21–65°N}} \approx \Delta\delta D_{\text{Antarctica}} \approx \delta D_{\text{Antarctica}} - \delta^{18}O_{\text{benthic}}$. This indicates that there is a "simple" relationship between climate changes in the high latitude region of the Southern Hemisphere and the mid-low latitude monsoon region of the Northern Hemisphere (Cheng et al., 2019). Thus, it is in fact possible to compare Asian speleothem $\delta^{18}O$ records to both Greenland and Antarctic ice core records.

It is widely accepted that ice core $\delta^{18}O$ records from Greenland and the Antarctic can be used as proxies of temperature. Hence, we directly compared the speleothem $\delta^{18}O$ records from the Asian monsoon region with those ice core $\delta^{18}O$ records in order to reveal the signal of the speleothem $\delta^{18}O$ records. Here, we compared the inverted speleothem $\delta^{18}O$ record (Hulu, Dongge and Sanbao caves) from the Asian monsoon region (Cheng et al., 2016) with the Greenland NGRIP $\delta^{18}O$ and the Antarctic EDC3 δD ice core records (North Greenland Ice Core Project members, 2004; Jouzel et al., 2007) during some periods. The results show that the inverted speleothem $\delta^{18}O$ composite record from the East Asian monsoon region, which receives sparse winter/spring precipitation, is similar to the Greenland NGRIP $\delta^{18}O$ and the Antarctic EDC3 δD ice core records from 0 to 130 kyr BP (Supplementary Fig. 13). Note the inverted curve of millennial mean $\delta^{18}O_s$ records are correlated with the Antarctic EDC3 ice core δD records during periods of 0-130 kyr BP, with a correlation coefficient of −0.22, within a 0.05 confidence level; the inverted curve of centurial mean $\delta^{18}O_s$ records are correlated with Greenland NGRIP $\delta^{18}O$ records during periods of 0-130 kyr BP (Yuan et al., 2004), with a correlation coefficient of −0.35, within a 0.01 confidence level. Moreover, the variations in the inverted speleothem $\delta^{18}O$ record (Cheng et al., 2016) are highly similar to those in the Antarctic EDC3 δD record (Jouzel et al., 2007) during 240 to 334, 343 to 386, 394 to 462, and 603 to 640 kyr BP, with a correlation coefficient of −0.30, −0.65, −0.38, and −0.63, within a 0.05, 0.01, 0.05, and 0.05 confidence level (Supplementary Fig. 14). The results show that our reinterpretation of ice core $\delta^{18}O$ records in the monsoon domain can be applied to speleothem $\delta^{18}O$ records from the Asian monsoon region (Wang Y. et al., 2008; Sinha et al., 2011; Cheng et al., 2016; Kathayat et al., 2017; Yuan et al., 2004). Hence, we argued that the inverted speleothem $\delta^{18}O$ records from the Asian monsoon region can also reflect temperature on the centennial as well as the orbital time scales.

4.3. Implications of inverted $\delta^{18}O$ records

How can the inverted ice core and speleothem $\delta^{18}O$ records from the Asian monsoon region indicate surface temperature changes? First, it should be noted that it is the in-cloud temperatures (or condensation temperatures) that control condensation and isotope fractionation. These cannot be routinely measured, and so correlation with surface air temperatures are made in many studies (Clark and Fritz, 1997). This can be done since the trends of surface temperatures in most regions are similar to those of the in-cloud temperatures. In this study, in the tropical regions, intense summer monsoon onset involves the abrupt increase of convection (Risi et al., 2008). This involves the uplift of warm and humid marine moisture from the tropical ocean to the high troposphere where the relatively low summer cloud-top temperatures (Fig. 4l) (Cai and Tian, 2016) produce an enhanced Rayleigh fractionation, resulting in low water vapor $\delta^{18}O$ ($\delta^{18}O_v$) (Fig. 4p, and Fig. 5) values and subsequently low $\delta^{18}O_p$ values in monsoon precipitation (Fig. 4h) despite the high summer surface temperatures (Fig. 4d, and Fig. 5). The residual moisture is transported to higher latitudes by the summer monsoon circulation, and the uplift of the subsequent convection over the mountains causes the $\delta^{18}O_v$ values of the residual moisture to decrease further (Fig. 4o). The subsequent precipitation is also characterized by lower $\delta^{18}O_p$ values (Fig. 4g) (Yao et al., 2013; Yu et al., 2017). In addition, we find that the summer cloud-top temperatures over the region where uplifted precipitation occurs is also relatively low, such as in Lhasa (Fig. 4k), which also contributes to the lower $\delta^{18}O$ values in the rain produced by the residual moisture (Fig. 4o; Fig. 5). Thus, the relatively lower $\delta^{18}O$ values of summer precipitation in the monsoon region are controlled by the cloud-top temperatures, or strictly speaking, they are controlled by the in-cloud (condensation) temperatures, which is a key parameter of the Rayleigh fractionation equation. That the corresponding surface temperatures in summer are high (Fig. 4c, 4d) and thus inversely correlated with precipitation $\delta^{18}O$ in the monsoon region (Fig. 4g, 4h) are a secondary consideration. We further find that the cloud-top temperatures over Lhasa (Fig. 4k), Tuotuohe (Fig. 4j), and Delingha (Fig. 4i) in summer gradually increase as the moisture moves from the monsoon region to the non-monsoon region, which results in the summer water vapor $\delta^{18}O_v$ values increasing from south to north (Fig. 4g, 4f, 4e; Fig. 5). In addition, the monsoon circulation gradually weakens from south to north, where the westerlies and local moisture recycling gradually strengthen. The result is that the magnitude of the decrease in summer precipitation $\delta^{18}O$ values from the monsoon region to the non-monsoon region becomes smaller (Fig. 5).

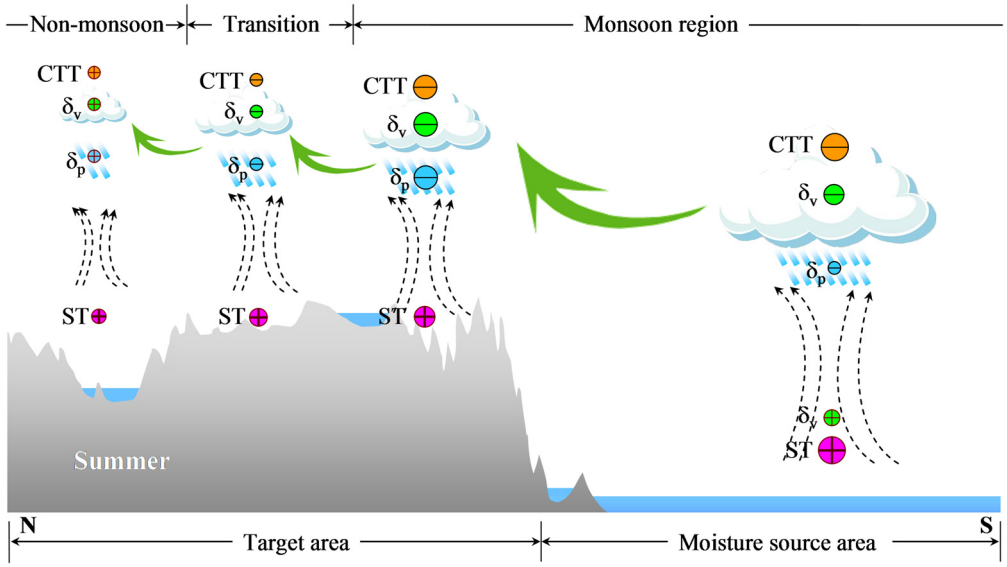

Fig. 5. Scheme illustrating how moisture is transported by the Asian monsoon (green arrow). Convection (dashed line with arrow), cloud-top temperature (CTT, yellow dot), water vapor δ_v (green dot), and surface temperature (ST, pink dot) all affect summer $\delta^{18}O_p$ (blue dot) from the ocean/coastal regions (moisture source area) to the Asian continent (target area). Note the minus (plus) signs within the circles that indicate decreased (increased) summer values, and the sizes of the circles show the magnitudes of those decreases (increases). The sizes of the green arrows and dashed lines indicate the relative strengths of the monsoon and convection.

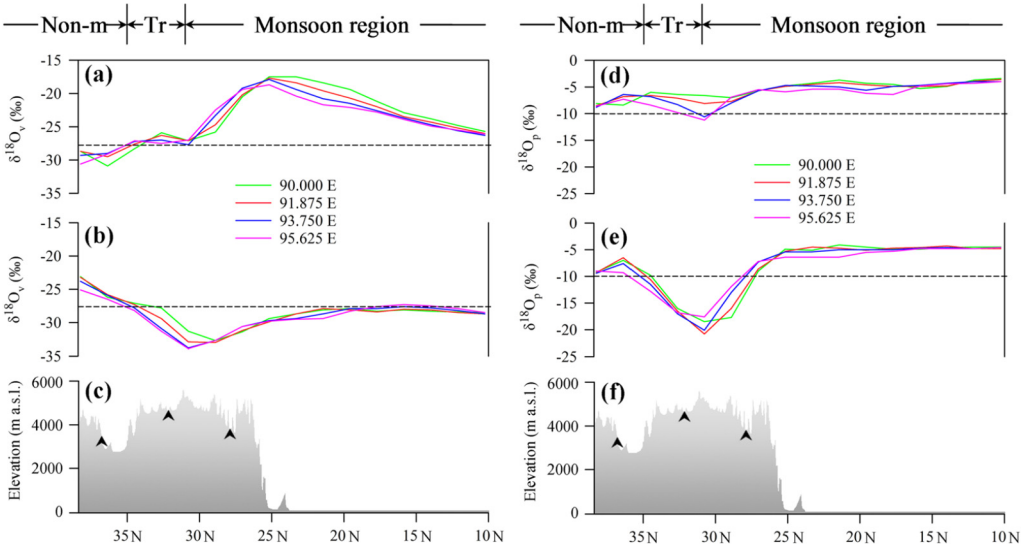

Fig. 6. North-south long-term mean simulated $\delta^{18}O_v$ (a, b) and $\delta^{18}O_p$ (d, e) profiles during 1979-1999 for May (pre-monsoon season) (a, d) and July (monsoon season) (b, e). Shadings show the topography cross-section profiles of the Tibetan Plateau (c, f). Note that the $\delta^{18}O_v$ at 500 hPa and the $\delta^{18}O_p$ are simulated by the ECHAM5-wiso model (Mutz et al., 2016). The $\delta^{18}O$ cross-sections at 90.000°E, 91.875°E, 93.750°E, and 95.625°E are marked by the green, red, blue, and pink lines, respectively. The black dashed lines indicate the reference values of −27.5‰ and −10‰ and are used to compare the $\delta^{18}O_v$ and $\delta^{18}O_p$ values in the monsoon season with those in the pre-monsoon season. The black arrows show the locations of the sampling stations of Lhasa (monsoon region), Tuotuohe (transition region, marked by Tr), and Delingha (non-monsoon region, marked by Non-m) from south to north, respectively. $\delta^{18}O$ is reported as per mil deviations from VSMOW or VSMOW2.

The ECHAM5-wiso (Mutz et al., 2016) simulations also demonstrate that the north-south (cross-sections at 90.000°E – 95.625°E) long-term mean $\delta^{18}O_v$ and $\delta^{18}O_p$ value profiles over the monsoon and transition regions of the Tibetan Plateau for July (monsoon season) are lower than those for May (pre-monsoon season), respectively (Fig. 6). Moreover, the $\delta^{18}O_v$ and $\delta^{18}O_p$ value shifts between the pre-monsoon and monsoon seasons from south to north are highly consistent with changes in cloud-top temperatures, respectively (Supplementary Figs. 8 and 9). Thus, the implications of $\delta^{18}O$, whether in ice cores, speleothems or in precipitation in the monsoon region and the non-monsoon region and at high or low altitude, can be explained by isotope fractionation.

The spatial correlation patterns between $\delta^{18}O_p$ and surface temperatures are shown in Fig. 7, based on the data from 120 stations in Asia (10°–50°N, 65°–130°E) (see Supplementary Table 3 for details). The ice core and speleothem $\delta^{18}O$ records from the regions north of the white line (that is affected by the westerlies and a weak monsoon) reflect surface temperature changes. Moreover, the temperature proxies of ice core and speleothem $\delta^{18}O$ records from the regions north of the black line, which are affected by intense westerlies, are defined by significant positive correlations of $\delta^{18}O_p$ – T (Supplementary Table 3). In the regions south of the white line, which are intensely affected by the monsoon, the $\delta^{18}O_p$ values are significantly negatively correlated with surface temperatures. In this case, ice core and speleothem $\delta^{18}O$ records may suggest the surface temperature changes in an inverse and indirect way, when the nearby meteorological stations are characterized by sparse precipitation in winter/spring.

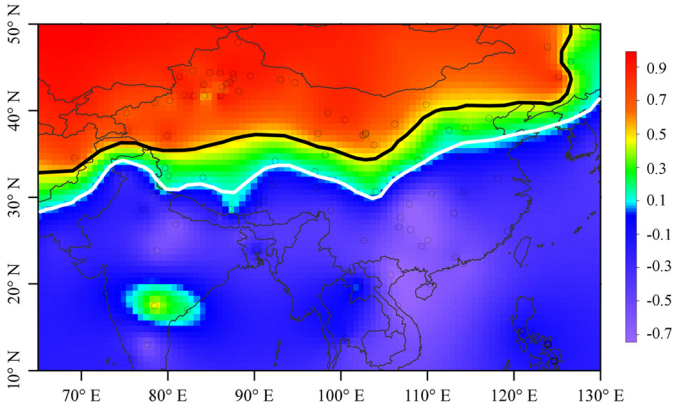

Fig. 7. Distribution of the correlation coefficients of $\delta^{18}O_p$–T in Asia. The distribution was calculated by the Kriging interpolation at 120 stations (open circles) in the region bounded by 10° to 50°N and 65° to 130°E. The area to the south of the white line is affected by intense summer monsoon, the region north of the black line is under the influence of intense westerlies, and the region between is transitional. Note the $\delta^{18}O$-T correlations are still significant in the transitional region between the white and black lines (see Supplementary Table 3 for details).

5. Conclusions

This study diagnosed the consistency of signals preserved in low-altitude precipitation $\delta^{18}O$ and high-altitude ice core $\delta^{18}O$. The results demonstrate that the trend changes in the $\delta^{18}O$ record at low altitude are consistent with those at high altitude. Clearly, the low-altitude $\delta^{18}O_p$ can capture the corresponding adjacent ice core $\delta^{18}O$ signals at high altitudes.

Our data show that the $\delta^{18}O_p$ values are consistently positively correlated with surface temperature in the non-monsoon and transition regions but are consistently inversely correlated with surface temperature in the monsoon region on different time scales. This implies that the $\delta^{18}O_p$ measurements and ice core $\delta^{18}O$ records from the non-monsoon and transition regions can directly indicate temperature, but they can "inversely" reflect temperature in the monsoon region. It indicates that ice core $\delta^{18}O$ records in the non-monsoon region can be used as a temperature proxy. In the monsoon region, if winter/spring precipitation is heavy, the ice core $\delta^{18}O$ records can still directly reflect temperature because temperature and $\delta^{18}O$ are more closely linked both in precipitation and in the ice core records. However, in the monsoon region, if winter/spring precipitation is sparse, the inverted ice core $\delta^{18}O$ records that agree with temperature will also reflect temperature changes. This results from the fact that trends of surface temperatures in the monsoon region are in contrast to the corresponding cloud-top temperatures, which controlled summer precipitation $\delta^{18}O$. Our findings also indicate that inverted curves of speleothem $\delta^{18}O$ records in the monsoon region are in accordance with the Greenland/Antarctic ice core $\delta^{18}O/\delta D$ and other paleotemperature records. This suggest that the inverted $\delta^{18}O$ records from Asian speleothems may also reflect temperature.

Here we demonstrate how temperature signals may have been preserved in stable isotope records from ice cores and speleothems from the Asian monsoon region. This study very clearly indicates that researchers need to be cautious when interpreting the ice core and speleothem $\delta^{18}O$ records from this region in the reconstruction of paleoclimate. Our findings suggest that in order to reconstruct temperature changes in the Asian monsoon region, ice core climate records from the regions where winter/spring precipitation is heavy may be more useful and their interpretation may depend in part on comparisons with inverted speleothem $\delta^{18}O$ records.

CRediT authorship contribution statement

Wusheng Yu: Conceptualization, Data curation, Investigation, Methodology, Software, Supervision, Visualization, Writing – original draft, Writing – review & editing. **Tandong Yao:** Writing – original draft. **Lonnie G. Thompson:** Writing – original draft, Writing – review & editing. **Jean Jouzel:** Writing – original draft, Writing – review & editing. **Huabiao Zhao:** Writing – original draft. **Baiqing Xu:** Writing – original draft. **Zhaowei Jing:** Data curation, Software, Writing – original draft. **Ninglian Wang:** Writing – original draft. **Guangjian Wu:** Writing – original draft. **Yaoming Ma:** Writing – original draft. **Jing Gao:** Writing – original draft. **Xiaoxin Yang:** Writing – original draft. **Jingyi Zhang:** Writing – original draft. **Dongmei Qu:** Writing – original draft.

Declaration of competing interest

The authors declare that they have no known competing financial interests or personal relationships that could have appeared to influence the work reported in this paper.

Acknowledgements

This research is supported by the CAS (XDA20060200), the National Key R&D Program of China (2017YFA0603303), and the NSFC (41671054, 41771085). Thanks go to Dr. Mary E. Davis (The Ohio State University, USA) for her valuable editing and comments. The authors acknowledge Dr. Sebastian G. Mutz (University of Tuebingen, Germany) for providing ECHAM5-wiso simulated isotopic data. Special thanks are given to two anonymous reviewers for their constructive comments. Some observed isotopic data used in this paper are from the IAEA/WMO Global Network of Isotopes in Precipitation (GNIP). Water vapor isotopic data derived from Tropospheric Emission Spectrometer (TES), onboard the NASA Aura satellite, were provided by NASA Langley Research Center Atmospheric Science Data Center. Some meteorological data were obtained from the Climatic Data Center, National Meteorological Information Center, China Meteorological Administration. NCEP reanalysis-derived data were obtained from the NOAA/OAR/ESRL PSD, Boulder, Colorado, USA. The TMPA data were provided by the NASA/Goddard Space Flight Center's Mesoscale Atmospheric Processes Laboratory and PPS, which develop and compute the TMPA as a contribution to TRMM. The ISCCP D1 and D2 products (cloud-top temperature, CTT) were obtained from NASA Goddard Institute for Space Studies. The data of the northern hemisphere temperature (CRUTEM4) were obtained from the Climatic Research Unit (University of East Anglia) and the Hadley Centre (UK Met Office).

Appendix. Supplementary material

Supplementary material related to this article can be found online at https://doi.org/10.1016/j.epsl.2020.116665.

References

Aggarwal, P.K., Romatschke, U., Araguas-Araguas, L., Belachew, D., Longstaffe, F.J., Berg, P., Schumacher, C., Funk, A., 2016. Proportions of convective and stratiform precipitation revealed in water isotope ratios. Nat. Geosci. 9, 624–629.

Berger, A., 1978. Long-term variations of caloric insolation resulting from earths orbital elements. Quat. Res. 9, 139–167.

Birks, S.J., Edwards, T.W.D., 2009. Atmospheric circulation controls on precipitation isotope–climate relations in western Canada. Tellus B 61, 566–576.

Cai, Y., Cheng, H., An, Z., Edwards, R.L., Wang, X., Tan, L., Wang, J., 2010. Large variations of oxygen isotopes in precipitation over south-central Tibet during Marine Isotope Stage 5. Geology 38, 243–246.

Cai, Z., Tian, L., 2016. Atmospheric controls on seasonal and interannual variations in the precipitation isotope in the East Asian monsoon region. J. Climate 29, 1339–1352.

Caley, T., Roche, D.M., Renssen, H., 2014. Orbital Asian summer monsoon dynamics revealed using an isotope-enabled global climate model. Nat. Commun. 5, 5371.
Chen, J.H., Rao, Z.G., Liu, J.B., Huang, W., Feng, S., Dong, G.H., Hu, Y., Xu, Q.H., Chen, F.H., 2016. On the timing of the East Asian summer monsoon maximum during the Holocene—Does the speleothem oxygen isotope record reflect monsoon rainfall variability? Sci. China Earth Sci. 59, 2328–2338.
Cheng, H., Edwards, R.L., Sinha, A., Spötl, C., Yi, L., Chen, S., Kelly, M., Kathayat, G., Wang, X., Li, X., Kong, X., Wang, Y., Ning, Y., Zhang, H., 2016. The Asian monsoon over the past 640,000 years and ice age terminations. Nature 534, 640–646.
Cheng, H., Zhang, H., Zhao, J., Li, H., Ning, Y., Kathayat, G., 2019. Chinese stalagmite paleoclimate researches: a review and perspective. Sci. China Earth Sci. 62, 1489–1513 (in Chinese).
Christiansen, B., Ljungqvist, F.C., 2012. The extra-tropical Northern Hemisphere temperature in the last two millennia: reconstructions of low-frequency variability. Clim. Past 8, 765–786.
Cobb, K.M., Adkins, J.F., Partin, J.W., Clark, B., 2007. Regional-scale climate influences on temporal variations of rainwater and cave dripwater oxygen isotopes in northern Borneo. Earth Planet. Sci. Lett. 263, 207–220.
Cosford, J., Qing, H., Mattey, D., Eglington, B., Zhang, M., 2009. Climatic and local effects on stalagmite $\delta^{13}C$ values at Lianhua Cave, China. Palaeogeogr. Palaeoclimatol. Palaeoecol. 280, 235–244.
Clark, I., Fritz, P., 1997. Environmental Isotopes in Hydrogeology. Lewis Publishers, Boca Raton, New York, p. 64.
Craig, H., 1961. Isotopic variations in meteoric waters. Science 133, 1702–1703.
Dansgaard, W., 1964. Stable isotopes in precipitation. Tellus 16, 436–468.
Dansgaard, W., Johnsen, S.J., Møller, J., Langway Jr., C.C., 1969. One thousand centuries of climatic record from Camp Century on the Greenland Ice Sheet. Science 166, 377–381.
Dansgaard, W., Johnsen, S.J., Clausen, H.B., Dahl-Jensen, D., Gundestrup, N.S., Hammer, C.U., Hvidberg, C.S., Steffensen, J.P., Sveinbjörnsdottir, A.E., Jouzel, J., Bond, G., 1993. Evidence for general instability of past climate from a 250-kyr ice-core record. Nature 364, 218–220.
Duan, W., Ruan, J., Luo, W., Li, T., Tian, L., Zeng, G., Zhang, D., Bai, Y., Li, J., Tao, T., Zhang, P., Baker, A., Tan, M., 2016. The transfer of seasonal isotopic variability between precipitation and drip water at eight caves in the monsoon regions of China. Geochim. Cosmochim. Acta 183, 250–266.
Gao, J., Risi, C., Masson-Delmotte, Y., He, V., Xu, B., 2016. Southern Tibetan Plateau ice core $\delta^{18}O$ reflects abrupt shifts in atmospheric circulation in the late 1970s. Clim. Dyn. 46, 291–302.
Goosse, H., Brovkin, V., Fichefet, T., Haarsma, R., Huybrechts, P., Jongma, J., Mouchet, A., Selten, F., Barriat, P.-Y., Campin, J.-M., Deleersnijder, E., Driesschaert, E., Goelzer, H., Janssens, I., Loutre, M.-F., Morales Maqueda, M.A., Opsteegh, T., Mathieu, P.-P., Munhoven, G., Pettersson, E.J., Renssen, H., Roche, D.M., Schaeffer, M., Tartinville, B., Timmermann, A., Weber, S.L., 2010. Description of the Earth system model of intermediate complexity LOVECLIM version 1.2. Geosci. Model Dev. 3, 603–633.
Guo, X., Tian, L., Wen, R., Yu, W., Qu, D., 2017. Controls of precipitation $\delta^{18}O$ on the northwestern Tibetan Plateau: a case study at Ngari station. Atmos. Res. 189, 141–151.
Hou, S., Qin, D., Zhang, D., Kang, S., Mayewskic, P.A., Waked, C.P., 2003. A 154a high-resolution ammonium record from the Rongbuk Glacier, north slope of Mt. Qomolangma (Everest), Tibet–Himal region. Atmos. Environ. 37, 721–729.
Hu, C., Henderson, G.M., Huang, J., Xie, S., Sun, Y., Johnson, K.R., 2008. Quantification of Holocene Asian monsoon rainfall from spatially separated cave records. Earth Planet. Sci. Lett. 266, 221–232.
Johnsen, S.J., Clausen, H.B., Dansgaard, W., Fuhrer, K., Gundestrup, N., Hammer, C.U., Iversen, P., Jouzel, J., Stauffer, B., Steffensen, J.P., 1992. Irregular glacial interstadials recorded in a new Greenland ice core. Nature 359, 311–313.
IAEA/WMO, 2018. Global network of isotopes in precipitation. The GNIP database. Accessible at http://www.iaea.org/water.
Jouzel, J., Lorius, C., Petit, J.R., Genthon, C., Barkov, N.I., Kotlyakov, V.M., Petrov, V.M., 1987. Vostok ice core: a continuous isotope temperature record over the last climatic cycle (160,000 years). Nature 329, 403–408.
Jouzel, J., Masson-Delmotte, V., Cattani, O., Dreyfus, G., Falourd, S., Hoffmann, G., Minster, B., Nouet, J., Barnola, J.M., Chappellaz, J., Fischer, H., Gallet, J.C., Johnsen, S., Leuenberger, M., Loulergue, L., Luethi, D., Oerter, H., Parrenin, F., Raisbeck, G., Raynaud, D., Schilt, A., Schwander, J., Selmo, E., Souchez, R., Spahni, R., Stauffer, B., Steffensen, J.P., Stenni, B., Stocker, T.F., Tison, J.L., Werner, M., Wolff, E.W., 2007. Orbital and millennial Antarctic climate variability over the last 800,000 years. Science 317, 793–796.
Kang, S., Zhang, Y., Zhang, Y., Grigholm, B., Kaspari, S., Qin, D., Ren, J., Mayewski, P., 2010. Variability of atmospheric dust loading over the central Tibetan Plateau based on ice core glaciochemistry. Atmos. Environ. 44, 2980–2989.
Kathayat, G., Cheng, H., Sinha, A., Yi, L., Li, X., Zhang, H., Li, H., Ning, Y., Lawrence Edwards, R., 2017. The Indian monsoon variability and civilization changes in the Indian subcontinent. Sci. Adv. 3, e1701296.
Kuo, T.S., Liu, Z.Q., Li, H.C., Wan, N.J., Shen, C.C., Ku, T.L., 2011. Climate and environmental changes during the past millennium in central western Guizhou, China as recorded by Stalagmite ZJD-21. J. Asian Earth Sci. 40, 1111–1120.
Li, J., Ehlers, T.A., Mutz, S.G., Steger, C., Paeth, H., Werner, M., Poulsen, C.J., Feng, R., 2016. Modern precipitation $\delta^{18}O$ and trajectory analysis over the Himalaya-Tibet Orogen from ECHAM5-wiso simulations. J. Geophys. Res., Atmos. 121, 10432–10452.
Li, Z., Feng, Q., Yong, S., Wang, Q.J., Jiao, Y., Li, Y., Li, J., Guo, X., 2016. Stable isotope composition of precipitation in the south and north slopes of Wushaoling Mountain, northwestern China. Atmos. Res. 182, 87–101.
Liu, W., Liu, W.Y., Li, P.J., Gao, L., Shen, Y.X., Wang, P.Y., Zhang, Y.P., Li, H.M., 2007. Using stable isotopes to determine sources of fog drip in a tropical seasonal rain forest of Xishuangbanna, SW China. Agric. For. Meteorol. 143, 80–91.
Liu, X., Liu, J., Chen, S., Chen, J., Zhang, X., Yan, J., Chen, F., 2020. New insights on Chinese cave $\delta^{18}O$ records and their paleoclimatic significance. Earth-Sci. Rev. 207. https://doi.org/10.1016/j.earscirev.2020.103216.
Majoube, M., 1971. Fractionnement en oxygène 18 et en deutérium entre l'eau et sa vapeur. J. Chim. Phys. Phys. Chim. Biol. 10, 1423–1436.
Moberg, A., Sonechkin, D.M., Holmgren, K., Datsenko, N.M., Karlén, W., 2005. Highly variable Northern Hemisphere temperatures reconstructed from low- and high-resolution proxy data. Nature 433, 613–617.
Mutz, S.G., Ehlers, T.A., Li, J., Steger, C., Paeth, H., Werner, M., Poulsen, C.J., 2016. Precipitation $\delta^{18}O$ over the Himalaya-Tibet orogen from ECHAM5-wiso simulations: statistical analysis of temperature, topography and precipitation. J. Geophys. Res., Atmos. 121, 9278–9300.
North Greenland Ice Core Project members, 2004. High-resolution record of Northern Hemisphere climate extending into the last interglacial period. Nature 431, 147–151.
Pang, H., Hou, S., Kaspari, S., Mayewski, P.A., 2014. Influence of regional precipitation patterns on stable isotopes in ice cores from the central Himalayas. Cryosphere 8, 289–301.
Pang, Z., Kong, Y., Froehlich, K., Huang, T., Yuan, L., Li, Z., Wang, F., 2011. Processes affecting isotopes in precipitation of an arid region. Tellus B 63, 352–359.
Rao, Z., Li, Y., Zhang, J., Jia, G., Chen, F., 2016. Investigating the long-term palaeoclimatic controls on the δD and $\delta^{18}O$ of precipitation during the Holocene in the Indian and East Asian monsoonal regions. Earth-Sci. Rev. 159, 292–305.
Risi, C., Bony, S., Vimeux, F., Descroix, L., Ibrahim, B., Lebreton, E., Mamadou, I., Sultan, B., 2008. What controls the isotopic composition of the African monsoon precipitation? Insights from event-based precipitation collected during the 2006 AMMA field campaign. Geophys. Res. Lett. 35. https://doi.org/10.1029/2008GL035920.
Roche, D.M., 2013. $\delta^{18}O$ water isotope in the *i*LOVECLIM model (version 1.0) – Part 1: implementation and verification. Geosci. Model Dev. 6, 1481–1491.
Sinha, A., Berkelhammer, M., Stott, L., Mudelsee, M., Cheng, H., Biswas, J., 2011. The leading mode of Indian Summer Monsoon precipitation variability during the last millennium. Geophys. Res. Lett. 38, L15703.
Takeuchi, N., Miyake, T., Nakazawa, F., Narita, H., Fujitat, K., Sakait, A., Nakawos, M., Fuji, Y., Duan, K., Yao, T., 2009. A shallow ice core re-drilled on the Dunde Ice Cap, western China: recent changes in the Asian high mountains. Environ. Res. Lett. 4, 045207.
Tan, L., Cai, Y., Cheng, H., An, Z., Edwards, R.L., 2009. Summer monsoon precipitation variations in central China over the past 750 years derived from a high-resolution absolute-dated stalagmite. Palaeogeogr. Palaeoclimatol. Palaeoecol. 280, 432–439.
Thompson, L.G., Mosley-Thompson, E., Davis, M.E., Bolzan, J.F., Dai, J., Yao, T., Gundestrup, N., Wu, X., Klein, L., Xie, Z., 1989. Holocene–late Pleistocene climatic ice core records from Qinghai–Tibetan Plateau. Science 246, 474–477.
Thompson, L.G., Yao, T., Davis, M.E., Henderson, K.A., Mosley-Thompson, E., Lin, P.-N., Beer, J., Synal, H.-A., Cole-Dai, J., Bolzan, J.F., 1997. Tropical climate instability: the last glacial cycle from a Qinghai-Tibetan ice core. Science 276, 1821–1825.
Thompson, L.G., Yao, T., Davis, M.E., Mosley-Thompson, E., Wu, G., Porter, S.E., Xu, B., Lin, P.-N., Wang, N., Beaudon, E., Duan, K., Sierra-Hernández, M.R., Kenny, D.V., 2018. Ice core records of climate variability on the Third Pole with emphasis on the Guliya ice cap, western Kunlun Mountains. Quat. Sci. Rev. 188, 1–14.
Thompson, L.G., Yao, T., Mosley-Thompson, E., Davis, M.E., Henderson, K.A., Lin, P.-N., 2000. A high-resolution millennial record of the South Asian Monsoon from Himalayan ice cores. Science 289, 1916–1919.
Tian, L., Yao, T., Li, Z., MacClune, K., Wu, G., Xu, B., Li, Y., Lu, A., Shen, Y., 2006. Recent rapid warming trend revealed from the isotopic record in Muztagata ice core, eastern Pamirs. J. Geophys. Res. 111, D13103.
Wang, N., Thompson, L.G., Davis, M.E., Mosley-Thompson, E., Yao, T., Pu, J., 2003. Influence of variations in NAO and SO on air temperature over the northern Tibetan Plateau as recorded by $\delta^{18}O$ in the Malan ice core. Geophys. Res. Lett. 30, 2167.
Wang, Y., Cheng, H., Edwards, R.L., Kong, X., Shao, X., Chen, S., Wu, J., Jiang, X., Wang, X., An, Z., 2008. Millennial- and orbital-scale changes in the East Asian monsoon over the past 224,000 years. Nature 451, 1090–1093.
Wang, P., Yao, T., Tian, L., Wu, G., Li, Z., Yang, W., 2008. Recent high-resolution glaciochemical record from a Dasuopu firn core of middle Himalayas. Chin. Sci. Bull. 53, 418–425.
Wang, S., Zhang, M., Hughes, C.E., Zhu, X., Dong, L., Ren, Z., Chen, F., 2016. Factors controlling stable isotope composition of precipitation in arid conditions: an observation network in the Tianshan Mountains, central Asia. Tellus B 68, 26206.

Werner, M., Langebroek, P.M., Carlsen, T., Herold, M., Lohmann, G., 2011. Stable water isotopes in the ECHAM5 general circulation model: toward high-resolution isotope modeling on a global scale. J. Geophys. Res. 116, D15109.

Worden, J., Noone, D., Galewsky, J., Bailey, A., Bowman, K., Brown, D., Hurley, J., Kulawik, S., Lee, J., Strong, M., 2011. Estimate of bias in Aura TES HDO/H_2O profiles from comparison of TES and in situ HDO/H_2O measurements at the Mauna Loa observatory. Atmos. Chem. Phys. 11, 4491–4503.

Yan, Y., Bender, M.L., Brook, E.J., Clifford, H.M., Kemeny, P.C., Kurbatov, A.V., Mackay, S., Mayewski, P.A., Ng, J., Severinghaus, J.P., Higgins, J.A., 2019. Two-million-year-old snapshots of atmospheric gases from Antarctic ice. Nature 574, 663–666.

Yao, T., Duan, K., Thompson, L.G., Wang, N., Tian, L., Xu, B., Wang, Y., Yu, W., 2007. Temperature variations over the past millennium on the Tibetan Plateau revealed by four ice cores. Ann. Glaciol. 46, 362–366.

Yao, T., Masson-Delmotte, V., Gao, J., Yu, W.S., Yang, X.X., Risi, C., Sturm, C., Werner, M., Zhao, H.B., He, Y., Ren, W., Tian, L.D., Shi, C.M., Hou, S.G., 2013. A review of climatic controls on $\delta^{18}O$ in precipitation over the Tibetan Plateau: observations and simulations. Rev. Geophys. 51, 525–548.

Yin, Q.Z., Berger, A., 2010. Insolation and CO_2 contribution to the interglacial climate before and after the Mid-Brunhes Event. Nat. Geosci. 3, 243–246.

Yu, W., Wei, F., Ma, Y., Liu, W., Zhang, Y., Luo, L., Tian, L., Xu, B., Qu, D., 2016. Stable isotope variations in precipitation over Deqin on the southeastern margin of the Tibetan Plateau during different seasons related to various meteorological factors and moisture sources. Atmos. Res. 170, 123–130.

Yu, W., Tian, L., Yao, T., Xu, B., Wei, F., Ma, Y., Zhu, H., Luo, L., Qu, D., 2017. Precipitation stable isotope records from the northern Hengduan Mountains in China capture signals of the winter India-Burma Trough and the Indian Summer Monsoon. Earth Planet. Sci. Lett. 477, 123–133.

Yuan, D.X., Cheng, H., Edwards, R.L., Dykoski, C.A., Kelly, M.J., Zhang, M., Qing, J., Lin, Y., Wang, Y., Wu, J., Dorale, J.A., An, Z., Cai, Y., 2004. Timing, duration, and transitions of the Last Interglacial Asian monsoon. Science 304, 575–578.

Zhao, H., Xu, B., Yao, T., Wu, G., Lin, S., Gao, J., Wang, M., 2012. Deuterium excess record in a southern Tibetan ice core and its potential climatic implications. Clim. Dyn. 38, 1791–1803.

Zhao, H., Xu, B., Li, Z., Wang, M., Li, J., Zhang, X., 2017. Abundant climatic information in water stable isotope record from a maritime glacier on southeastern Tibetan Plateau. Clim. Dyn. 48, 1161–1171.